Networks and Spatial Economics (2023) 23:679–713
https://doi.org/10.1007/s11067-023-09592-1

Dynamic Wireless Charging Facility Location Problem for Battery Electric Vehicles under Electricity Constraint

Amit Kumar[1] · **Sabyasachee Mishra**[2] · **Huan Ngo**[2]

Accepted: 23 May 2023 / Published online: 17 June 2023

Abstract
Despite the recent development in technology, Battery Electric Vehicle (BEV) pose several drawbacks including recharging time, limited range, and inadequate number of charging facilities. In an effort to address these drawbacks, Dynamic Wireless Charging (DWC) technology is gaining attention. DWC can be implemented by embedding the induction coil under a roadway pavement to dynamically charge the BEV in motion without a need to stop. This prompts an important question for infrastructure planning of BEVs: how to optimally locate DWC infrastructure in a road network. Planning for optimal DWC facility location needs to consider how BEV drivers will react to the newly implemented DWC in terms of route choice to reflect their unilateral utility minimization objective. Further complexities of DWC implementation include availability of zonal surplus electricity. In this paper, we propose a bi-level planning approach considering both the objectives of the planners and the drivers. The approach explicitly incorporates five elements: system-level social costs, travel patterns of individuals, trip completion assurance, zonal DWC implementation constraint due to energy availability from grid, and total budget availability from the public agency. The proposed framework is first demonstrated in a numerical experiment setting using Sioux Falls network. Then the framework is also implemented using city of Chicago sketch network to demonstrate its applicability to real-size networks. The numerical results using these two networks provide valuable insights for planners for developing an optimal DWC implementation plan.

Keywords Surplus electricity · Regional energy availability, Transportation electrification · Range constraint · Inductance-based charging

1 Introduction

In the United States, greenhouse gas emission has been one of the major issues in recent years and the transportation sector is responsible for 29% of the total emission since it uses approximately 29% of the total energy and operates based mainly

Extended author information available on the last page of the article

on fossil fuel, which has a 92% share among other alternatives (USDOE 2018). These emissions are generated from the process of burning fossil fuel from Internal Combustion Engine Vehicles (ICEV). In contrast to ICEV, Battery Electric Vehicles (BEV) present a solution for alleviating the current state of emission since BEV uses electric motor for which electricity can be produced by greener sources like solar, hydro and nuclear in contrast to ICEVs that burns fuel to generate propulsion force. Moreover, the combination of superior fuel economy efficiency over ICEV, relatively low maintenance cost, and tax incentives at Federal and State levels makes BEV more appealing to consumers. However, the adoption of BEV has two main disadvantages compared to ICEV that deters its market penetration: (i) range constraint leading to range anxiety and (ii) long recharging time leading to extended charging downtime.

The BEV driving range is defined as the furthest distance a BEV can travel using the full state of charge (SOC) of its battery-pack without the need of refueling. Despite recent developments in battery technology the average driving range of BEV have been able to reach 190 miles. In addition, assuming fuel capacity of 20 gallons and fuel economy of 23 miles per gallon, an ICEV has driving range of 460 miles which is more than twice as compared to BEV. In addition, like ICEV fuel tank is typically not always full, BEV's SOC is not 100%. While the gas stations are abundant the charging stations are scarcely located. This results in range anxiety which limits the adoption of BEV because travelers are afraid that the vehicle's SOC would not provide enough range to reach destination (Agrawal et al. 2016).

BEV's motors are powered by high-capacity batteries which are typically charged by plugging it into an electric charging point. This conventional plug-in recharging method suffers from two disadvantages: the BEV is nonoperational during the recharging time, which is referred to as charging downtime (Hwang et al. 2018), and extended recharging time. An ICEV with 20 gallons gas tank capacity can be refueled within 2–3 min at a gas dispense rate of 5–10 gallons per minute. In addition, BEV requires at least 25 min to be fully recharged even at the highest level of charging (Liu and Wang 2017). The super charging stations with 960 kW or above in power can bring the charging time to 5 min recharging time for a 200-mile range BEV however, they are impractical given the current charging technology (Fuller 2016). This leads to an extended charging downtime for BEVs.

To address these two issues related to BEV, researchers have proposed induction based dynamic wireless charging (DWC). DWC facility works like electric transformer where the primary induction coil is embedded under a roadway pavement that can inductively charge the BEV's battery through the secondary coil sitting in vehicles lower part of body while in motion. DWC can potentially reduce or may even eliminate the BEV's charging downtime. Moreover, a proper DWC implementation in a road-network can satisfy the range requirement of BEVs operating in the network and help to relieve range anxiety. However, existing infrastructure and electricity availability must also be addressed when integrating DWC since it is still a new concept. DWC facility demands a certain amount of available electricity in order to be practically beneficial to the public such as reducing range anxiety and addressing charging downtime drawback. It prompts the question on whether or not the existing electricity system can support such demand on top of the current

industrial and commercial electricity consumption. Therefore, the location and length of DWC Facility within a network, referred as the DWC Facility Location Problem (DWC-FLP), needs to be planned optimally under multiple constraints to derive its maximum benefit and ultimately promote the cleaner transportation through adoption of BEV.

There has been a growing interest in DWC in recent past as evident from pertinent literature addressing the DWC-FLP (Dong et al. 2014; García-Vázquez et al. 2017; He et al. 2018; Jang 2018; Panchal et al. 2018). However, previous studies in DWC related literature generally consider only the transportation planners' objectives, ignore the regional surplus electricity available for DWC and apply the framework to small-scale network. However, there are other analogous research in the domain of FLP although not focusing on DWC, such as on refueling station location in networks (Kuby and Lim 2005), and FLP for surveillance of network for planning purposes (Matisziw 2019) that consider both planer's and network users objectives and consider real-scale network. Therefore, the objective of this paper is to develop an enhanced planning framework, which is capable of solving large scale real-world network, to optimally determine the location and length of DWC facility in a road network for BEV while simultaneously considering the following elements: government planning objective, driver's behavior, reduce range anxiety, the availability of electricity and planning agency's budget constraint.

The rest of the paper is organized as follows. The Section 2 discusses literature on the optimal deployment of DWC facility and BEV users driving behavior. The Section 3 presents modeling approach and numerical experiments using a small-scale network. The Section 4 presents case study and solves the DWC-FLP for the travel demand and network data for City of Chicago, Illinois, USA to test the model applicability for practice and draw inferences from the model's results. The final section discusses the overall performance of the model, its limitations, and avenues for future research.

2 Literature Review

This section summarizes pertinent literature of facility location problems in the context of BEV. The past literature falls into two categories which are optimal location of DWC facilities and network flow estimation considering driver behavior. We review the literature in these two categories, identify the research gap, and provide the corresponding contribution of this research.

2.1 Optimal Location of Charging Facility

Past literature is extensive especially on the topic of charging/refueling location problem for BEVs (or alternate fuel vehicles (AFV)). Huang et al. (2015) proposes a refueling location model by considering the behaviors of AFV users who are willing to deviate slightly from their most preferred routes to ensure that their AFVs with limited travel ranges can be refueled en-route to their destinations. Zheng et al. (2017) investigated the BEV traffic equilibrium and optimal deployment of charging

locations subject to range limitation. Jang (2018) conducted a survey on the operation and system issues aspect of wireless charging namely dynamic and quasi-dynamic and suggested that the wireless charging systems prompt new questions with regards to allocation of charging facilities, cost and benefit analysis, and billing and pricing. Panchal et al. (2018) reviewed multiple aspects of the wireless electric vehicle charging system such as method of charging, wireless transformer topologies, health and safety standards. Dong et al. (2014) examined the infrastructure cost for implementing DWC which takes into account the vehicle and charging system, specification and cost of integration into existing roadway. In addition, BEVs also differ to ICEVs in fuel efficiency. García-Vázquez et al. (2017) developed a model to compare the electricity consumption on three different stretches which are motorway, highway and urban. The model considers the area of Cadiz, Spain and their results suggest that BEV energy consumption may fluctuate greatly in urban areas whereas on highways it may be more stable. He et al. (2018) created a modified electricity consumption model to assess the effect of DWC on link travel time and they applied it on a two-lane DWC system.

Later studies cover commercial use of recharging facility for private automobiles. Zhang et al. (2017) considered a capacitated flow and multi-period approach for locating static supercharging for BEVs while including user demand dynamics resulting from charging opportunities prompting from newly implemented facilities. Chen et al. (2016) provided a problem for the optimal deployment of DWC in a road network with user equilibrium under trip completion assurance for BEVs. Dong et al. (2014) created a multi-level static charging plan for BEV using an activity based approach. Their approach simulates the driver travel and recharging pattern based on the GPS travel survey in the greater Seattle area and create charging plan by minimizing BEV driver range anxiety measured as number of interrupted trips and uncompleted vehicle miles. Sathaye and Kelley (2013) created a plan for charging infrastructure for plug-in electric vehicles with an objective of minimizing budget in terms of public fund while accounting for existing private entity charging infrastructure and fluctuation of user demand within the Texas Triangle megaregion. Liu and Wang (2017) formulated a Tri-Level model which considers simultaneously the following tasks: planning agency's decision for DWC facility location, users vehicle type choice which can be either a plug-in electric vehicle or a full battery electric vehicle, and users route choice for their specific trips. For the upper-level optimization problem, they adopt a weighted minimization objective function of total system travel time and normalized penalty because of failed trips. The decision about whether or not to implement DWC for a specific road is reflected by model output in the form of binary decision variable. The study demonstrates the model application using Nguyen-Dupuis and Sioux Falls test networks. Riemann et al. (2015) proposed a bi-level approach for DWC location problem in which the upper level maximizes the amount of traffic flow served by the DWC facilities and the lower-level determines network flow using Multinomial Logit based Stochastic User Equilibrium principle.

Liu et al. (2017) and Liu and Song (2017) proposed a framework for deciding the optimal location of the DWC facilities and designing the optimal battery sizes of electric buses for an electric bus system. However, there are four fundamental

differences between this study and that proposed by Liu and Song (2017). First, we propose a framework for deciding the optimal location of DWC facility in a transportation network for private vehicles while that by Liu and Song (2017) proposed it for electric bus network. The buses operate on fixed route while private vehicles' (cars') drivers are free to decide their route and select their route based on travel cost minimization. Hence, decision of DWC location impacts path choice of BEV drivers but it's not true for bus network. Second, we proposed a bi-level optimization to incorporate BEV driver's path choice at lower level while Liu and Song (2017) used a single level optimization that minimizes total system cost. Third, we consider zonal power availability constraint in deciding the DWC location that is not considered in Liu and Song (2017). Fourth, we adopt a continuous decision variable that can take any value between 0 and 1 in contrast to binary decision variable adopted in Liu and Song (2017).

2.2 Estimation of Network Flows and Route Decision by BEV Drivers

The planning agency makes the decision about the location of facilities (for example charging facility) along the various routes in a transportation network. The BEV drivers typically consider the charging locations in addition to travel cost in route choice process choose the route that maximizes their utility. These decisions by network users (drivers) collectively affect travel times in a network and determines the traffic flow as well. In literature, the aggregate route choice decisions resulting in network level flows are often incorporated at the lower-level problem representing network user perspective. The literature in this domain indicates that majority of studies focuses on the problem of estimating network flows under charging facility and range constraint. Xie et al. (2017) proposed a path-constrained traffic assignment problem for BEV considering stochastic driving ranges. Their research concentrated on the tour or trip chaining where customer range anxiety is more likely to occur. The BEV's SOC may be a non-linear function of recharging time in comparison to ICEV refueling which is a linear function of fueling time. To address this issue, Montoya et al. (2017) suggested a hybrid metaheuristic for BEV routing problem that takes into account components developed in earlier studies and specifically designed components using the non-linear behavior of BEV recharging. Zhang et al. (2019) proposed to model the traffic assignment of mixed-vehicular traffic of PEVs with two different charging capabilities accounting for PEV range constraints. Liu et al. (2016) proposed a model for better fuel efficiency for BEVs by utilizing a realistic drive cycle based on the GPS logs of paths travelled by electric vehicles in California. Strehler et al. (2017) determined the shortest path for battery electric and hybrid vehicle by considering several factors that are not typically considered in the shortest path problem of ICEVs including extended recharging time, the tradeoff between range and speed, and regenerative braking. There has been also effort to develop combined mode choice and route choice models. For example, Kitthamkesorn and Chen (2017) analyzed the coupled model that includes mode choice and traffic assignment by utilizing a nested Weibit model for mode choice path-size Weibit model for route choice and demonstrated its superior performance

compared to logit models. A BEV driver's utility (and hence route choice) may also be impacted by level of improvement of state of charge (amount of electricity recharged) along the route with links enabled with DWC. However, this factor has not been considered in majority of past studies related to route choice of BEV drivers and estimation network flows.

2.3 Contribution and Significance of This Study

In the literature, the majority of the studies focus on lower level of the bi-level problem which is BEV traffic assignment. There are few studies focused on optimal DWC facility plan. However, typically these studies have not considered amount of electricity recharged by DWC facility and are restricted to small size networks owing to expense of computational complexity. In addition, majority of studies focusing on optimal DWC facility location problem using bi-level approach generally consider binary decision variable representing whether or not to implement DWC on the entire length of a link under consideration. An important limitation of using binary decision variable is that it provides less flexibility and does not allow to implement DWC on a part of a link and leading to a sub-optimal solution in particular for a network containing long links e.g., access-controlled facilities (interstate highways and long arterials). Specifically, implementing DWC on an entire length of a highway would be an inefficient use of resources. A counter intuitive argument here can be that this issue can be addressed by considering the highway as a collection of multiple smaller links. However, this argument leads to another issue on how to get the optimal lengths of segments for the original links. Recognizing these gaps in literature Ngo et al. (2020) proposed a model for DWC location problem considering electricity recharged by DWC facility and a continuous decision variable representing a portion of the link in the bi-level optimization model. However, in their study similar to past studies, network is treated as a whole which restricts the model's ability to account for zonal availability of electricity supply. Further Ngo et al. (2020) in their study assumed that there is always sufficient power to meet the energy demand by DWC so that all failed paths can be avoided. However, for real-size (large) city networks, there might not be surplus power to meet the electricity demand for DWC to avoid all failed trips. Hence there is need to relax the failed path constraint and account for zonal electricity availability constraint.

This study endeavors to bridge these gaps identified in the literature. There are two important theoretical contributions of this study. First, we incorporate zonal power availability constraint for DWC planning after meeting domestic, commercial, and industrial electricity demand. Second, our formulation tends to minimize the number of failed trips due to insufficient charge of BEV's battery by range augmentation through DWC. We further relax these two constraints for applicability of the model to real-size networks. We explicitly incorporate five important elements into our approach which are: system-level network social costs, travel patterns of individuals, an effort to limit the number of failed path (trip completion assurance), zonal DWC implementation constraint either due to energy availability from grid in an electrical district, and total agency budget. And to the best of our knowledge,

all of these five elements have not yet been considered in the literature simultaneously. Akin to past studies, we develop a sequential bi-level optimization approach considering the objectives of the government agency and BEV drivers at upper and lower levels respectively. The numerical experiments are conducted using data for two real-size networks to gain insights for practical applications. Proposed framework is first demonstrated on a small Sioux Falls network then real-world application are conducted using the City of Chicago network developed by the Chicago Area Transportation Study (Boyce et al. 1985). The inferences from these numerical experiments can benefit the practitioners and planners greatly in developing a DWC infrastructure investment plan, within a given budget while minimizing the social cost and energy consumption.

3 Methodology

3.1 Modeling Approach

In this study the DWC facility location problem is modeled as bi-level optimization problem. In the Upper-Level (UL) we incorporate the planning agency and government perspectives. A government/ planning agency has objectives of maximizing the social benefits resulting from infrastructure investments. In this case we assume that objective of planning agency for the implementation of DWC facilities is to minimize the network-level total social cost while ensuring that the required resources for the implementation does not exceed the agency budget. However, such a viewpoint cannot encapsulate different microscopic interpretation of the network users benefiting from DWC facility. The government agency can get information on traffic flow and travel time, by methods such as travel surveys, passive data, or a four-step transportation planning process. Based on the existing data of traffic flow and travel time, a typical approach for implementing DWC facility would be to locate it on links that carry maximum traffic flows so that more BEVs can be recharged. However, drivers react in accordance with the newly implemented DWC, and in this case, drivers will prefer the DWC implemented roads. Thus, the road may get congested resulting in travel delay, which is not ideal. The approach of using the existing network flow data, which does not account for the variation in the network flows due to proposed facility location, would not yield the optimal result intended for planning. This necessitates feedback to UL problem about impact on network condition due to aggregate network user response to DWC-FLP plan.

In the Lower-Level (LL) we consider the variation in network flow resulting from the government's DWC Location Plan that reflects network users' collective route choice behavior assuming network consists of only BEV drivers. Assuming rational driver behavior users chose their path by maximizing their utility (or a minimum disutility). The users' disutility is incorporated in the form of normalized travel time. The normalized travel time represents the aggregate of the following elements: (1) summation of travel time of the links included in the chosen path (disutility), and (2) the aggregate benefit to BEV in the form of improvement of their battery's SOC as it receives charge by DWC facilities while they are driven along chosen path

in the DWC implemented network. The improvement in SOC may be considered as positive utility (or negative disutility) for a path. However, the link travel times and hence energy recharged received through DWC are also the functions of link flows. This is due the fact that energy transferred to BEV through DWC will depend on aggregate time a BEV stays over the primary coil embedded on the links of network. In this study, we assume that link times (travel costs) are separable and link travel time depends on the flow of that link only. A higher flow on a link will result in higher travel time but also higher energy transferred to BEV through DWC and hence higher SOC benefit on that link leading to higher range augmentation of BEV. Therefore, BEV drivers are likely to have a trade-off between travel time (a disutility) and SOC improvement or range augmentation through DWC (a negative disutility). We formulate DWC-FLP as bi-level optimization problem, and Fig. 1 depicts the relationship between the UL and LL problems and their dependencies while showing the information exchange between two levels.

Notations

To schematically describe the UL and LL MP formulations, we introduce the following notations and parameters used in the model:

Sets

A Set of links

W Set of Origin–Destination pairs

P_w Set of paths for O–D pair w

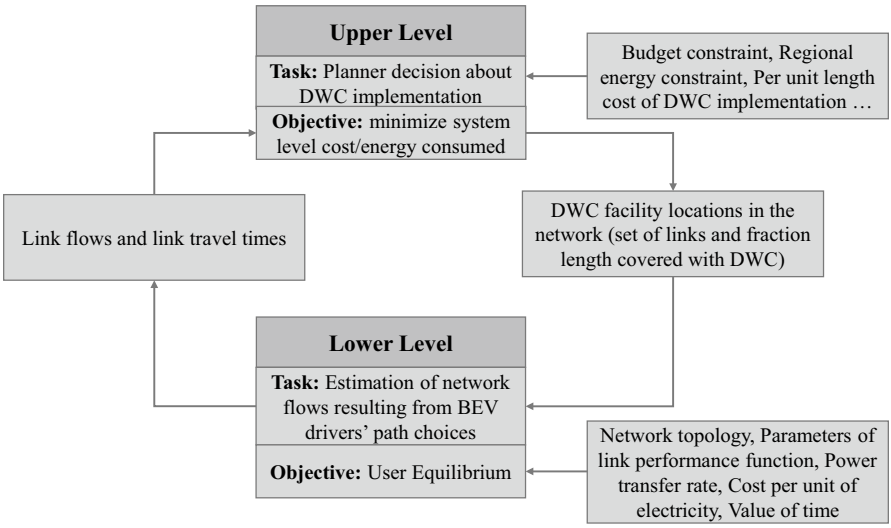

Fig. 1 Upper and Lower-Level Relationship

Q Set of regions

Parameters

b Cost of implementing dynamic wireless charging facilities (in Million $/mile)$\theta$Agency budget

r Rate of range augmentation per unit time spent on DWC facility by BEV (in miles/minute)

ψ Power transfer rate by DWC facility (in kW)

η Cost of one unit of electricity (in $/kWh)

τ Value of time (in $/h)

E Constant for electricity constraint

K Constant for failed paths constraint

l_a Length of link a

μ_a Negative cost experienced by the driver due to DWC recharging along link a (in travel time units, i.e., minutes)

l_a^e Length of link a having DWC charging facility (in mile)

cap_a Capacity of link a

t_a^0 Free flow travel time on link a

t_a Travel time on link a

g_a Generalized cost for traveling on link a

α_a Coefficient α specifically for link a in the link cost (BPR) function

β_a Coefficient β specifically for link a in the BPR function

s_a Average speed on link a (in miles per hour)

ϖ_a Average fuel efficiency on link a (in miles per kWh)

γ_a Energy consumption rate for traversing link a (in kWh)

ε_p Vehicle start range using path p

rem_p Remaining range of vehicle on path p

q_w Total travel demand of O-D pair w

δ_{ap}^{w} Link-path incident parameter, which takes the value 1 if link a belongs to path p of O-D pair w and 0 for otherwise

f_p^w Flow on path p of the O-D pair w

C_m Predefined constant for maximum DWC facilities (as total length) in an area Q_m

ζ_m Fraction reflects zonal surplus electricity

π Parameter of sigmoid function (positive real number)

$\%elec_m$ Total non-transportation electricity consumption of area m as a percentage of total electricity consumption

Decision Variables

y_a Length of DWC facility on link a as a percentage of the length of link a

v_a Flow on link a

κ_p Variable representing whether a path p fails or not

3.2 Upper-Level of Government Decision Making

At the upper level of the bi-level problem, we consider two different performance measurement objectives from planners' perspective, first to quantify the network level social cost in the form of Total System Travel Time (TSTT) and second to quantify the network level energy efficiency in the form of Total System Energy Consumption (TSEC). The first objective, TSTT can be calculated by taking the aggregate sum of (all links within the network) link flows multiplied by travel time. TSTT is a frequently used metric in network infrastructure investment studies. The second objective, TSEC is determined by taking the aggregate sum of (all links in the network) link flows multiplied by average energy consumption for BEVs while traversing that link.

Model 1: Minimizing total system travel time (TSTT)
Objective Function:

$$\min z_1 = \sum_{a \epsilon A} v_a t_a \tag{1}$$

Subject to:

$$b \sum_{a \epsilon A} y_a l_a \leq \theta \tag{2}$$

$$\varepsilon_p + \sum_{a \in p} (r y_a t_a - l_a) \geq 0 \forall p \in P_w, w \in W \tag{3}$$

$$0 \leq y_a \leq 1 \forall a \in A \tag{4}$$

$$t_a = t_a^0 \left[1 + \alpha_a \left(\frac{v_a}{cap_a} \right)^{\beta_a} \right] \forall a \in A \tag{5}$$

$$v_a = f(y_a) \tag{6}$$

$$g_a = t_a + \mu_a v_a \geq 0 \tag{7}$$

The objective function of Model-1 is represented by Eq. (1) that minimizes the total system travel time. The traffic flow (v_a) in objective function depends on the UL decision variable, the DWC plan represented by vector [y_a]. The travel time (t_a) in objective function depends on the traffic flow (v_a). Even though the UL decision variable [y_a], is not explicitly present in the objective function, it necessarily affects the objective function value through network users' response. Equation (2) states that the total cost of implementing DWC within the network must not exceed the agency budget. We further make a simplifying assumption that all vehicles selecting a path p between an O-D pair has a same starting range ε_p. Equation (3) ensures that BEVs' battery gets sufficient charge through DWC to complete their trips. In other words, Eq. (3) ensures that there are no failed trips in the network due to BEV running out of charge. The second term in Eq. (3) represents the range augmented from recharging through DWC facility. In power industry power transfer is measured in kW. Multiplying power transfer rate through DWC with the time spent by a BEV over the DWC facility, we get the amount of energy in terms of electricity transferred to the BEV. However, as the second term in Eq. (3) is in distance unit, we utilize the average BEV electricity consumption rate measured in Wh/mile to convert it to the equivalent range. For simplification, we introduce a coefficient r that represents the additional range gained by BEV per minutes of travel over DWC facility. With a 120 kW DWC power transfer rate and a 400 Wh/Mile average fuel economy of BEV, the value of r is 5 miles/min travel. Equation (4) defines the range of decision variable y_a. In this study we assume that it is a continuous variable representing

the length of the DWC facility in a link expressed as the percentage link length and represented as a fraction (hence it lies in closed interval between 0 and 1). Equation (5) represents the link performance function (this study uses the BPR function) that establishes the relation between link travel time (t_a) and link flow (v_a). Where, t_a^0 is the free flow travel time and α_a, β_a, cap_a are the parameters of link cost function specific to link a. Equation (6) implies traffic flow (v_a) is a function of DWC plan [y_a]. Taking the output of UL [y_a] as the input the LL determines link flows satisfying User Equilibrium. However, there is no mathematical function relating these two variables. Equation (7) avoids circular paths by ensuring that no link has negative generalized cost.

We add a local electricity constraint which is meant to avoid overloading the local electrical network due to excessive power demand by DWC facilities within a district. The installation of DWC facilities on the links in a district is restrained by a predefined constant. To illustrate this constraint, let Q_m, represents a district in a study area $\boldsymbol{Q}$ having q mutually exclusive districts, then,

$$Q_1 \cup Q_2 \cup Q_3 \cdots \cup Q_m \cup \cdots \cup Q_q = \boldsymbol{Q},\ and\ Q_m \cap Q_n = \varnothing \forall Q_m, Q_n$$

Let the set of links that fall in the district Q_m is represented as A_m and for each Q_m there is a predefined constant C_m representing surplus electric power from grid after meeting the domestic, commercial and industrial demands. Then the Zonal DWC implementation constraint can be defined as follows:

$$\sum_{a \in A_m} y_a l_a \leq C_m \forall Q_m \in Q \tag{8}$$

Equation (8) states that the total DWC implemented in an electrical district must be less than a predefined constant C_m for that district. Equation (8) assumes that a link is part of only one district Q_m and hence $A_m \cap A_n = \varnothing$. However, this assumption is not restrictive, and in cases of long links extending to multiple districts, we can split the link into multiple links each spanning in one district only. This will be typically the case for long arterials and interstate highways. Later we relax failed path constraint and zonal DWC constraint represented by Eqs. (3) and (8) for applicability of the model to real-size networks.

Model 2: Minimizing total system energy consumption (TSEC)

Objective Function:

$$\min z_2 = \sum_{a \epsilon A} v_a \gamma_a \tag{9}$$

Subject to:

$$s_a = l_a / t_a \forall a \in A \tag{10}$$

$$f_a = h(s_a) \forall a \in A \tag{11}$$

$$\gamma_a = l_a / \varpi_a \forall a \in A \tag{12}$$

and constraint represented by Eqs. (2)–(8)

Equation (9) represents the objective function of the second scenario which is to minimize the total system energy consumption. The Model 2 is also subjected to the constraints listed in Model 1. Equation (10) gives the average speed of vehicles traversing on link a of length l_a and travel time t_a. Equation (11) describes the relationship between fuel economy of a link and the average speed. We suggest this relationship to be in a form of a quadratic function defined as $h(s_a) = \alpha_0 + \alpha_1 s_a + \alpha_2 s_a^2$. Equation (12) calculates the energy consumption for a BEV traveling on link a.

3.3 Lower-level Network User Equilibrium

The task of determination of network flows (paths/links flows) resulting due the network users' path choice decisions as the aggregate response to DWC implementation plan of planners are often referred to as a traffic assignment problem. Traffic assignment can be categorized as either static or dynamic traffic assignment. Static assignment assumes that traffic is in a steady-state and hence flows and travel times of links can be represented using average conditions. Because of its simple mathematical formulation and solution procedure, the static assignment is widely applied for planning applications. Wardrop's User equilibrium (UE) principle, which assumes that users reach equilibrium when they cannot improve their travel time (cost) unilaterally by switching routes, is mostly used for finding the network flows in a transportation network. According to Sheffi (Sheffi 1985), the deterministic user equilibrium traffic assignment problem can be formulated as a convex optimization problem. In the context of this study, we use the following MP formulation for single class BEV static deterministic user equilibrium (BEV-UE) problem by customizing the BEV-UE formulation proposed by Ngo et al. (2020) for a DWC implemented network.

BEV-UE:
Objective Function:

$$\min z_3 = \sum_{a \in A} \left(\int_0^{v_a} t_a(x_a)\,dx + \mu_a v_a \right) \tag{13}$$

Subject to:

$$\sum_k f_p^w = q_w, \quad \forall w \in W \tag{14}$$

$$v_a = \sum_{w \in W} \sum_{p \in P_w} \delta_{ap}^w f_p^w, \ \forall a \in A \tag{15}$$

$$f_p^w \geq 0, \forall p \in P_w, \ w \in W \tag{16}$$

$$\mu_a = -\frac{l_a^e}{s_a}\psi\eta\left(\frac{60}{\tau}\right), \forall a \in A \tag{17}$$

$$l_a^e = y_a l_a, \ \forall a \in A \tag{18}$$

Equations (13)–(18) represents the BEV-UE formulation under the DWC facility. Equation (13) is a minimization of the objective function. Equation (14) defines flow conservation. Equation (15) defines the relationship between link and path flow. Equation (16) ensures path flows are non-negative. Equation (17) characterizes the negative cost of BEV drivers because of DWC. Equation (18) determines the DWC length on a link and relates UL decision variables to LL problem. Here, it is imperative to mention the difference between MP formulation proposed by Ngo et al. (2020) and that used here. The difference lies in fact that while in BEV-UE proposed by Ngo et al. (2020) the power transfer to BEV through DWC on a link is assumed to be proportional to length of a link implemented with DWC, in this study we assume that power transfer to BEV through DWC on a link is proportional to time traveled on DWC implemented portion of link. Hence, owing to congestion effect, higher the link volume, slower is the average speed, higher is the power transfer. In BEV-UE formulation of Ngo et al. (2020) the effect of congestion on power transfer to BEVs through DWC is ignored.

Next, we show that MP formulation represented by Eqs. (13)–(18) represents BEV-UE. For this purpose, we construct the Lagrangian of the minimization problem as follows:

$$\mathcal{L}(\boldsymbol{f}, \boldsymbol{\sigma}) = z_3(\boldsymbol{f}) + \sum_{w \in \boldsymbol{W}} \sigma_w \left[q_w - \sum_{p \in \boldsymbol{P}_w} f_p^w \right] \tag{19}$$

where, σ_w is the Lagrange multiplier for equality constraint in Eq. (14). Note that definitional constraints (Eqs. (13)–(18)) do not enter in the Lagrange function $\mathcal{L}(.)$. At the stationary point of Lagrangian, the following three conditions need to be satisfied in addition to non-negativity constraints:

$$f_p^w \frac{\partial \mathcal{L}}{\partial f_p^w} = 0, \forall p \in \boldsymbol{P}^w, w \in \boldsymbol{W} \tag{20}$$

$$\frac{\partial \mathcal{L}}{\partial f_p^w} \geq 0, \forall p \in \boldsymbol{P}^w, w \in \boldsymbol{W} \tag{21}$$

$$\frac{\partial \mathcal{L}}{\partial \sigma_w} = 0, \forall w \in \boldsymbol{W} \tag{22}$$

Noting the fact that partial derivate of x_a with respect to f_p^w is δ_{ap}^w, and using diagonal rule, the partial derivatives of z_3 with respect to f_p^w is given as:

$$\begin{aligned}\frac{\partial z_3}{\partial f_p^w} &= \frac{\partial z_3}{\partial x_a}\frac{\partial x_a}{\partial f_p^w} \\ &= \sum_{a\in A}\left(t_a + \mu_a\right)\delta_{ap}^w \\ &= \sum_{a\in A}\left(g_a\right)\delta_{ap}^w = G_p^w\end{aligned} \tag{23}$$

where, g_a and G_p^w are the generalized cost of traveling on link a and path p respectively. Using above information the partial derivatives of $\mathcal{L}(.)$ with respect to f_p^w is given as:

$$\frac{\partial \mathcal{L}}{\partial f_p^w} = \frac{\partial}{\partial f_p^w} z_3(\boldsymbol{f}) - \sigma_w = G_p^w - \sigma_w \tag{24}$$

Using the stationarity conditions (20–22) we obtain:

$$f_p^w(G_p^w - \sigma_w) = 0, \forall p \in \boldsymbol{P}^w, w \in \boldsymbol{W} \tag{25}$$

$$G_p^w - \sigma_w \geq 0, \forall p \in \boldsymbol{P}^w, w \in \boldsymbol{W} \tag{26}$$

Considering σ_w as the minimum generalized path cost for the O-D pair w above two Eqs. (24) and (25) together imply Wardopian User Equilibrium of BEVs.

3.4 Upper-Level Model Modification for Real-World Application

There are major differences in network characteristic between a small test network (like Sioux Falls network used in the numerical experiment section) and the real-size networks (for example Chicago network in the real-world application section). In small network, there is an assumption that there is enough budget to implement DWC so that all failed trips are avoided. However, it is not the case of large and complex networks where the budget needed to cover all trips would be enormous. Besides the budget assumption, small networks can strictly restrain the DWC facility due to local energy availability. In contrast, in large networks, it may be acceptable to relax the energy availability constraint to achieve overall benefit of the network users. In particular, some constraints if applied simultaneously can reduce the feasible solution space drastically thereby making the search of optimal solution difficult, the numerical experiment under such condition is neither feasible nor practical when applied to the real-world networks. There are two specific constraints that fall into this particular criterion. The first constraint is the trip completion assurance (no failed paths) constraint represented by Eq. (3) and the second is the Zonal DWC implementation constraint represented by Eq. (8).

First, we relax the no failed paths constraint in Eq. (3) for the two reasons: (1) given the limited budget, it is not plausible to guarantee that all paths can be covered with DWC ensuring no failed path, (2) some of the paths are utilized by a few drivers or even not utilized at all, thus it may be a waste of budget to invest on those

paths especially under low agency budget. To address this, we modify the failed paths constraint so that the total number of failed paths must not exceed an upper limit. Each path is attributed with a binary variable κ_p stating if it fails or not:

$$\kappa_p = \begin{cases} 1 \ if \ \varepsilon_p + \sum_{a \in p}(ry_a t_a - l_a) < 0 \\ 0 \ if \ \varepsilon_p + \sum_{a \in p}(ry_a t_a - l_a) \geq 0 \end{cases} \forall p \in P_w, w \in W$$

However, the use of binary variable is computationally difficult for larger networks and therefore we linearize the variable with a set of equations as follows:

$$rem_p = \varepsilon_p + \sum_{a \in p} \left(ry_a t_a - l_a\right) \ \forall p \in P_w, w \in W \tag{27}$$

$$\kappa_p = \frac{1}{1 + e^{\pi * rem_p}} \forall p \in P_w, w \in W \tag{28}$$

$$\sum_{w \in W} \sum_{pa \in P_w} \kappa_p \leq K \tag{29}$$

Equation (19) gives the remaining range rem_p of the vehicle traveling along path p. A positive rem_p value indicates that the path is covered by any BEV using it and negative otherwise. Equation (20) represents the sigmoid function where if rem_p is negative, κ_p would take the value approximately to 1 and 0 otherwise. The parameter π is a positive (real number) constant for sigmoid function. Equation (21) states that the sum of failed paths must be less than a pre-defined constant K. For applicability to large networks, the electricity constraint in Eq. (8) is relaxed to reflect the situation where a DWC plan in an electrical district can deviate from its pre-defined constant. In particular, for large network, we relax the constraint (8) by so that BEV charging through DWC do not over-utilize the electric system in an electrical district which already experiences high commercial/industrial consumption, and relaxed constraint is represented using Eqs. (22)–(23) as follows:

$$\sum_{Q_m \in \boldsymbol{Q}} \left(\frac{\sum_{a \in A_m} y_a l_a}{\sum_{a \in A} y_a l_a} - \zeta_m \right)^2 \leq E \tag{30}$$

$$\zeta_m = \frac{(1 - \%elec_m)}{\sum_{Q_m \in \boldsymbol{Q}} (1 - \%elec_m)} \forall Q_m \in \boldsymbol{Q} \tag{31}$$

Constraint in Eq. (22) is based on the sum of the squares of differences between two terms. The first term is the total DWC implemented in an electrical district Q_m expressed as a percentage of total DWC implemented in the entire network (entire area Q), and the second term ζ_m reflects zonal surplus electricity. This sum of square

must be less than a pre-defined constant E. Equation (23) states that ζ_m changes in opposite direction to the total domestic, industrial, and commercial electricity consumption in a community denoted by $\%elec_m$ in an area Q_m. ζ_m is measured in percentage of available energy in an area so that ζ_m sum up to "one" over the entire area Q. Although from power grid planning perspective total energy requirement can be computed from vehicle miles traveled by BEV and its energy efficiency, they cannot provide power demand surge due to DWC at the district level. Zonal grid constraint represented by Eqs. (22) and (23) tend to minimize the zonal imbalance of power demand surge due to DWC while ensuring that total power demand from DWC does not exceed the available power at the network level.

3.5 Solution Algorithms

The Bi-Level program considered in this study presents a problem of an expensive black-box objective function optimization. The term expensive black-box objective function refers to the circumstances when the following two criteria appear concurrently: (1) the decision variable is not present in the objective function regardless of its strong impact on the value of the objective function; and (2) the objective function value can only be calculated via a different optimization process. In our upper-level problem, the decision variable, which is the length and location of DWC facilities, and the value of the objective function (TSTT or TSEC) are not related to each other in an explicit mathematical manner. The value of the objective function can only be obtained after executing the traffic assignment problem to obtain the travel time and flow of each link in the LL problem. The bi-level programming is known to be NP-hard (Ben-Ayed and Blair 1990; Deng 1998). In order to solve this black-box objective function optimization, we utilize and extend the Constrained Local Metric Stochastic Response Surface (ConstrLMSRS) algorithm proposed by Regis (2011). The algorithm works as a feedback loop until convergence. It consists of three steps: initialization, exploration, and conclusion. The main advantages of this algorithm are two-fold: (1) despite solving the traffic assignment problem (LL problem) for each candidate point within an iteration, it is computed for only the best candidate point per iteration resulting in a significant reduction in computational cost, and (2) it allows decision variables to be continuous to better represent the flexibility of implementing DWC facilities. The step size used in the modified ConstrLMSRS is also continuous to sufficiently cover all the possible solutions. We use ConstrLMSRS algorithm to analyse real-world networks with reasonable computational cost, however, other algorithms such as Memetic Algorithm (Pishvaee et al. 2010), Differential Evolution (Koh 2007), Evolutionary Algorithms (Lau et al. 2009) and Hill climbing (Los and Lardinois 1982) can also be explored. The psuedo code is provided below:

Solution Algorithm for Upper-Level Problem

Stage 1. Initialization

Step 1.1. Create a set of initial *N* training points which satisfies all constraints of the optimization problem $X_0 = \{x_1, x_2 \ldots x_n\}$. These points do not need to yield the optimal results. Each training points x_n has a dimension of Å which represents cardinality of *A since in our formulation, the upper-level decision variable is the percentage of DWC on various links and its dimension should be same as A*.

Step 1.2. Calculate the objective function of each training points using the expensive objective function $Z = \{\mathrm{f}(x_1), \mathrm{f}(x_2) \ldots \mathrm{f}(x_n)\}$. Sort for the minimum value of the: $Z_{best} = \min(Z)$ at x_{best}.

Set 1.3. Set the initial step size $\theta_g = \theta_{initial}$; Consecutive Success and Failure: $C_{succ} = 0$; $C_{fail} = 0$; and global successive failure $C_{gsf} = 0$

Stage 2. Exploration. Let *g* be the index for each global episode (or iteration).

While the termination condition ($g > G_{max}$ *or* $C_{gsf} > C_{gsfmax}$) is not satisfied do the following:

Step 2.1. Using the training points $N = \{(x_1, \mathrm{f}(x_1)), (x_2, \mathrm{f}(x_2)) \ldots (x_t, \mathrm{f}(x_t))\}$ create or update the response surface $S_g(x)$. The response surface is used to interpolate the objective function value.

Step 2.2. Generate *p* candidates points for each iteration *g*: $C_g = \{x_{g,1}, \ldots x_{g,p}\}$ as follow: For *j =1 ...p:*

Generate Å uniform random number $w_1, w_2 \ldots w_n$ in the range [0,1]. Let $I_{pert} = \{i: w_i < prob_{sltc}\}$. If $I_{pert} = \emptyset$, then select *j* from the set [1, … , Å] and set $I_{pert} = \{j\}$

Generate *j*-th candidate solution by: $x_{g,1} = x_{best} + \Delta_{g,j}$ where $\Delta^i_{g,j}$=0 for all $i \notin I_{pert}$ and $\Delta^i_{g,j}$ is a normal random variable with mean 0 and standard deviation θ_g for all $i \in I_{pert}$

Step 2.3. For each candidate point $x_{g,j} \in C_g$

If the candidate point $x_{g,j}$ satisfy all constraints within the optimization,

Determine the objective function $S_g(x_{g,j})$ by using the response surface model.

Let $S^{min} = \min\{S_g(x_{g,j}), x_{g,j} \in C_g\}$ and $S^{max} = \max\{S_g(x_{g,j}), x_{g,j} \in C_g\}$. Calculate the score for each $x_{g,j} \in C_g$ for the response surface: if $S^{max} \neq S^{min}$ then $V_g^S = (S_g(x_{g,j}) - S^{min})/(S^{max} - S^{min})$, else $V_g^S = 1$.

Determine the minimum distance from the candidate $x_{g,j}$ to training points by $D_g(x_{g,j}) = min_{1 \le i \le g} \left|\left|x_{g,j} - x_i\right|\right|, x_i \in Z$. The symbol $||.||$ describes the Euclidean norm. Let $D^{min} = \min\{D_g(x_{g,j}), x_{g,j} \in C_g\}$ and $D^{max} = \max\{D_g(x_{g,j}), x_{g,j} \in C_g\}$. Calculate the score for distance criterion score for each candidate: if $D^{max} \neq D^{min}$ then $V_g^D = (D_g(x_{g,j}) - D^{min})/(D^{max} - D^{min})$ else $D_g^S = 1$.

Step 2.4. Calculate the weighted score for each candidate points: $V_g = w_g^S V_g^S + w_g^D V_g^D$. The coefficient w_g^S, w_g^D can be determined as follow: $w_g^S = \begin{cases} v_{mod(g-g_0,k)} & if\ mod(g-g_0,k) \neq 0 \\ v_k & otherwise \end{cases}$ and $w_g^D = 1 - w_g^S$ where *k* is an integer and v_k is a series of weights in ascending order within the range of [0,1]. Select x^* within the set of candidates points C_g that yields the highest weighted score V_g.

Step 2.5. Compute the expensive objective function for the solution x^* to get the value $Z_g = \mathrm{f}(x^*)$ and add the point $\{x^*, \mathrm{f}(x^*)\}$ to the training points poll *N*. Calculate the accuracy of the response surface model by: $acc_{S_g} = \left|S_g(x^*) - \mathrm{f}(x^*)\right|$

Step 2.6. If $Z_g < Z_{best}$ update the current best solution $Z_{best} = Z_g$, update the consecutive success and failures: $C_{succ} = C_{succ} + 1$; $C_{fail} = 0$; $C_{gsf} = 0$ otherwise $C_{fail} = C_{fail} + 1$; $C_{succ} = 0$.

Step 2.7. Adjusting the step size and counters:

If C_{succ} exceeds the maximum number of successes C_{succ}^{max}, set $\theta_{n+1} = \theta_n/2$ and reset $C_{succ} = 0$

If C_{fail} exceeds the maximum number of successes C_{fail}^{max}, set $\theta_{n+1} = 2\theta_n$, reset $C_{fail} = 0$, and set $C_{gsf} = C_{gsf} + 1$

Set *n = n+1*

End of while loop.

Step 3. Termination

Return the optimal objective function value Z_{best} and the vector of decision variable $\{y_{best}\}$ when stopping criterion is met. The stopping criterion adopted is either the iteration reaches 150 iterations or global successive failure reaches 10.

The LL problem (BEV-UE) is solved by customizing the SPSA algorithm proposed by Kumar and Peeta (2014a). The customization aims to incorporate generalized cost including negative cost owing to DWC charging. The customized algorithm is a path-based algorithm, and it decomposes the solution process into two steps: construct a restricted master problem (RMP) and find an equilibrium solution for the RMP. The construction of RMP in the present context involves identification of the set of UE paths which is not known a priori and is constructed assuming free flow conditions in network and updated iteratively. In addition, based on insights from Kumar et al. (2012) it updates the RMP using simultaneous strategy (simultaneously updates the path sets for all O-D pairs) and solves the RMP using origin based strategy. The customized algorithm is labeled as Simultaneous RMP update Origin-Based flow update Algorithm (S-RMP-OBA).

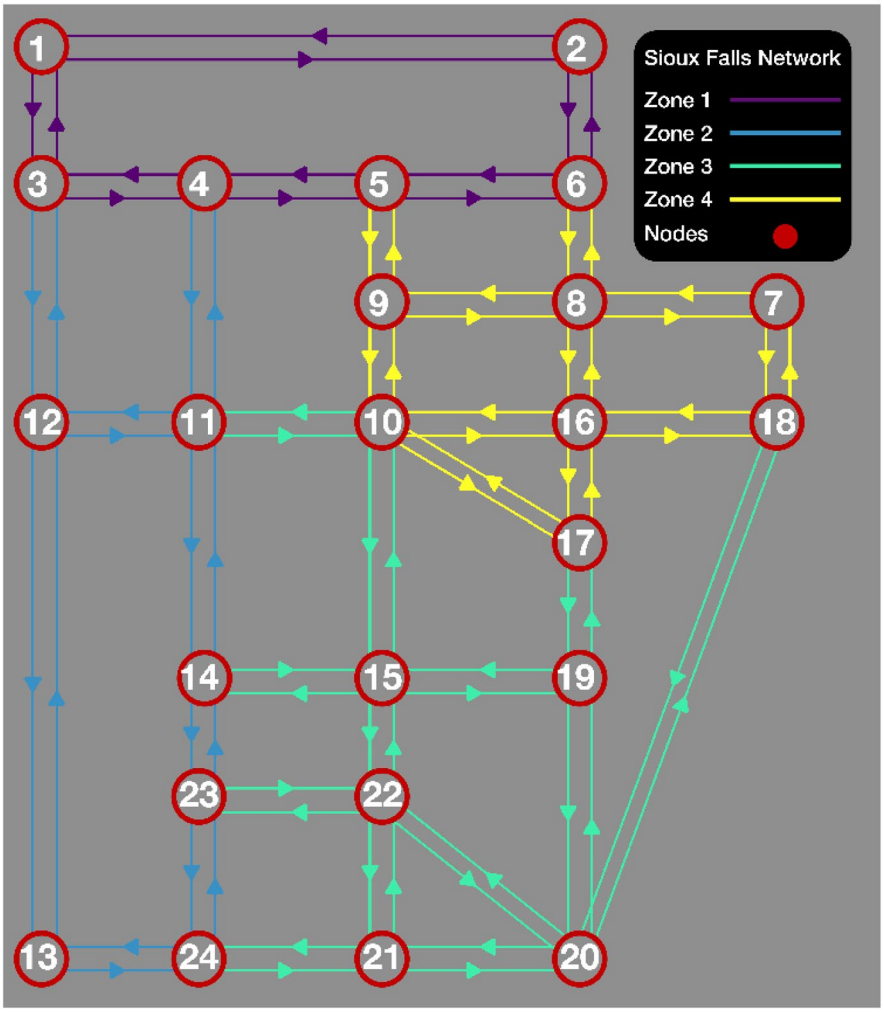

Fig. 2 Sioux Falls Network

S-RMP-OBA has been implemented using C++ code. This implementation also takes insights from Kumar and Peeta (2014b) to improve the link flow and link cost update processes in the iterative solution process. The S-RMP-OBA provides link flows and travel times at user equilibrium which acts as input to the UL problem. The implementation steps of S-RMP-OBA are presented here.

Solution Algorithm for Lower-Level (S-RMP OBA) BEV-UE Model

The steps of solution procedure for solving the BEV-UE Model are as follows:

Step 0: Initialization: Initialize the network by assigning OD demand to shortest paths of network. Set *iter*=1.

Step 1: Update link parameters, link travel time and generalized link costs for each link (using parallel processing).

Step 2: Update path sets P_w for all OD pairs (Simultaneous Approach) for the network using following steps (parallel processing applicable as various OD based trees are independent of each other):

Step 2.1: Go to first origin.

Step 2.2: Update path sets for all OD pairs rooted at this origin as follows:

(a) Generate shortest paths for all OD pairs rooted at this origin and update generalized path costs G_p^w for all paths in the existing path sets of these OD pairs.

(b) If a generated path is not present in the path set assign zero flows to that path and add the generated path to respective path set (for the given OD pair of the network).

Step 2.3: If this is last origin then go to step 3, otherwise, go to next origin and Step 2.2.

Step 3: Find the move direction for path flow updates and update paths flows, followed by link flows and link costs using origin-based approach.

Step 3.1: Go to first origin.

Step 3.2: Go to first destination from this origin. Initialize path flow $f_{p,old}^w = f_p^w \; \forall p \in P_w$

Step 3.2.1: Find the move directions for this OD pair:

(a) Compute shift factor for each path $p \in P_w$, with respect to all other paths $l \in P_w$ for this OD pair as follows:

$$\varrho_{p,l}^w = \begin{cases} (G_l^w - G_p^w) * f_l \,, if \;\; G_l^w > G_p^w \\ -(G_p^w - G_l^w) * f_p \,, if \;\; G_p^w > G_l^w \end{cases} , \forall p \in P_w$$

(b) The path move factor for path p is given as: $d_p^w = \sum_{l \in P_w} \varrho_{p,l}^w$

(c) The move direction is given as $\boldsymbol{d}^w = [d_k^w]$

Step 3.2.2: Compute step size λ_{iter} using line search.

Step 3.2.3: Update flows of paths as: $[f_p^w] \leftarrow [f_{p,old}^w] + \lambda_{iter} \boldsymbol{d}^w$.

Step 3.2.4: Check for violation of feasible region and project path flows to feasible region if violated using following steps:

(a) if path flow $f_p^w < 0$, then set $\lambda_{old}^w = \lambda_{iter}$ and compute new candidate step size as follows:

$$\lambda_{j,new}^w = \frac{-f_j^w}{d_j^w} + \lambda_{old}^w \;, \forall j: \left(j \in P^w \;\&\; f_j^w < 0\right)$$

(b) Compute maximum step size as: $\lambda max_{iter} = \min_j (\lambda_{j,new}^w)$

(c) Update flows of paths as: $[f_p^w] \leftarrow [f_{p,old}^w] + \lambda max_{iter} \boldsymbol{d}^w$.

Step 3.2.5: Update link flows and link costs similar to step 1.

Step 3.2.6: If this is last destination then go to step 4 else go to next destination from this origin, update path costs for this OD pair and then, go to Step 3.2.1.

Step 4: If this is last origin then go to Step 5 otherwise, go to next origin and then go to Step 3.2.

Step 5: Check termination criteria. If satisfied, then stop else update $iter \leftarrow iter + 1$ and go to Step 2. The termination criteria used in this study is (i) Relative gap (*Rgap*) with termination threshold 1.0E-08 computed as:

$$Rgap = \frac{\sum_w \sum_k c_k^w f_k^w - \sum_w \sum_k c_*^w f_k^w}{\sum_w \sum_k c_k^w f_k^w}$$

4 Numerical Study Using a Small Network

4.1 Sioux Falls Network

The proposed framework is first applied to Sioux Falls network, a small-scale network. This helps to demonstrate the numerical analysis on DWC implementation plan. The network consists of 24 nodes, all of which are origin and destination nodes, 76 links, and 360,900 trips (in Vehicles/Day). Sioux Falls has frequently been used in numerous studies (Leblanc 1975; Lee et al. 2014; He et al. 2015; Huang and Li (n.d.); Kumar and Mishra 2018; Kumar et al. 2019; Haque et al. 2021). In addition to the original data, we assign network links to 4 different electrical districts based on their location. This assignment is meant to address the local DWC implementation constraint due to electricity availability. Figure 2 shows the topography of the network. The links are color-coded to represent their designated electrical zone (district). This zonal distribution is not same as traffic analysis zone (TAZ).

The study makes following simplifying assumptions: (1) the cost of implementing DWC is $4 million per lane per mile and the agency budget is $65 million, (2) all vehicle have a starting range of 10 miles, (3) the problem is considered as an uncapacitated refueling model which states that there is no limitation on the number of vehicles being charged at a time, (4) all vehicles are BEV capable of recharging through a DWC facility thereby able to increase its range by traveling over links installed with DWC, and (5) the pre-defined constants C_m for each zone are equal to 4.07 miles.

4.2 Model Training

The Sioux Falls Case Study is executed in a Dell Precision Tower which has an Intel Core i7-6700 CPU at 3.40 GHz with 8 CPUs and 16 GB of RAM. The upper-level is scripted in MATLAB version R2019a and the lower-level is modeled and optimized in C++. We run both model TSTT and TSEC for 100 iterations and store the real value of the objective function. With these settings, the model completed training in 218.4 and 207.5 min for the TSTT and TSEC respectively. In the solving algorithm, the model is utilizing the Radial Basis Function to estimate the black-box objective function value instead of solving for the complicated User Equilibrium. This process is applied to every candidate solution points and thus it effectively reduces the training time by a significant margin.

Figure 3a, b show the real objective function value of TSTT and TSEC respectively. In the beginning, both models have only small improvement in the objective function. This can be attributed to two reasons. First, the initial training points have already covered a wide range of solutions and the first best value is reasonably low that it is hard for the algorithm to improve upon. Second, given the assumption of range and budget, the feasibility region of the model is very small that there is little difference between the set of candidate feasible solutions. However, both TSTT and TSEC see an improvement in the middle of the

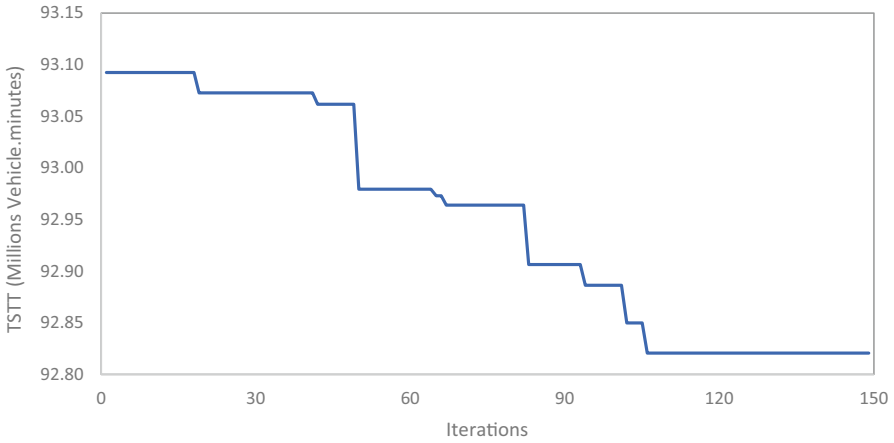

(a) TSTT objective function by iteration

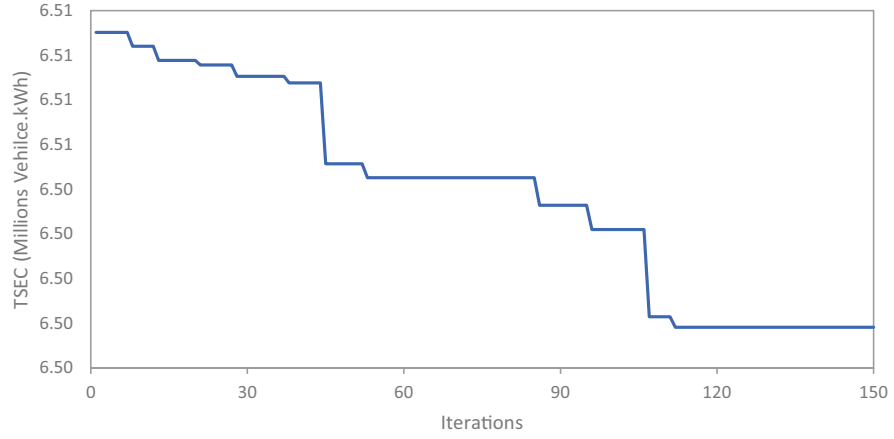

(b) TSEC objective function by iteration

Fig. 3 Objective function by iteration

training period which indicates the algorithm explores new area of the feasibility region. This happened at iteration 46th and 50th respectively. The same phenomenon is repeated near the end of the training at the 84th and 96th iteration. The training reaches non-improving objective function or convergence at iteration 108th and 112th for TSTT and TSEC and the algorithm is stopped by the termination criteria. On average, the running time of the lower level is 87.3 s.

4.3 Model Output and Insights

The results of numerical experiment of DWC implementation plan for the Sioux Falls Network are presented in Fig. 4 depicting the spatial location and extent of DWC facility. Figure 4a, b show the results for the TSTT and TSEC model scenarios

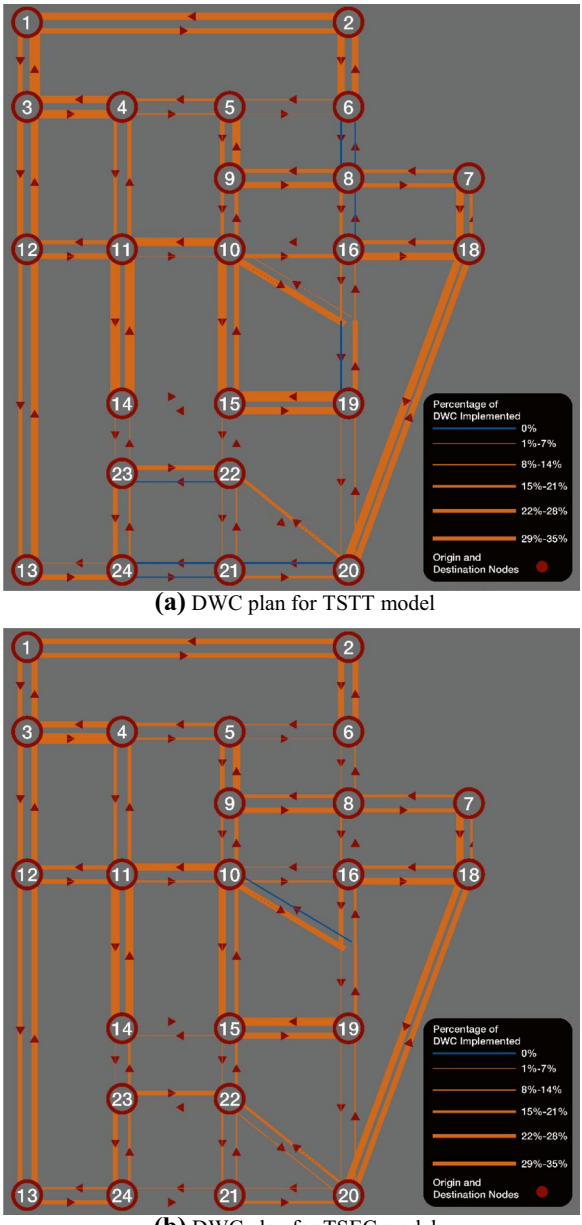

(a) DWC plan for TSTT model

(b) DWC plan for TSEC model

Fig. 4 DWC Implementation Plan for Sioux Falls Network

respectively. The line thickness in these figures represent the extent (fraction of link length) of DWC implementation suggested by proposed framework. The results for TSTT scenario indicate that DWCs are implemented more heavily in selected links which results in several links not receiving any DWC treatment. In contrast, in TSEC model resulted in DWC allocation in a well distributed manner covering most of

Fig. 5 Chicago Network Characteristic ▶

the links excluding one. The differences between two scenarios are attributed to the nature of objective function considered by the planning agency. The common DWC allocated links between two models are the critical links serving majority of traffic in the network and these links provide the recharging facility for multiple paths and ultimately multiple trips. The numerical results show that the proposed model can be applied for DWC facility allocation with decision makers' objective as TSTT or TSEC subjected to various infrastructure and electricity availability constraints.

5 Real World Application

5.1 City of Chicago Network

The methodology proposed in this study has also been applied to the City of Chicago network located in Illinois, USA, as the case study to obtain further insights on strengths and limitations of the proposed model for a large network. The City of Chicago network is based on the Chicago Regional network developed by the Chicago Area Transportation Study (Boyce et al. 1985). The Chicago Regional network, which consists of 12,982 nodes, 39,018 links, actually extends beyond Chicago city onto other rural areas. For computational flexibility and anticipating low population density, rural areas are excluded from the original Chicago network. The City of Chicago network used in this case study application, only considers the nodes, links, and trips within the political region of Chicago city with the anticipation that DWC can provide services to more users.

Chicago is the third-largest city in the United States which is home to approximately 2.7 million residents. The network has 3 main highways running across the city which are Interstate 90, 55, and 290. Among these 3 highways, Interstate 90 is more important for two reasons: first, it provides access to the Central Business District (CBD) for residents located in both the Southern and Northern part of Chicago and second it connects the CBD to the O'Hare International Airport. Besides these highways, travelers also utilize major arterials such as the South Lake Shore Drive which runs North–South of the city and along the Michigan Lake, and North Milwaukee Avenue which runs East–West. In addition, the majority of the local road aligns in either the North–South or East–West direction which provides easy navigation for drivers who do not have access to GPS assistance. The City of Chicago is divided into 77 community areas and this division was first introduced by the Social Science Research Committee at the University of Chicago in 1920 (Burgess and Newcomb 1920). In addition to Census tract, these community areas are introduced for statistical and planning purposes because it is a better representation of native neighborhoods in Chicago. These community areas are separated by physical barrier (e.g., river, railroad, etc.) which then necessarily forms a distinct identity. In relation to our model, these community areas are the small district Q_m and facilitate the zonal DWC electricity

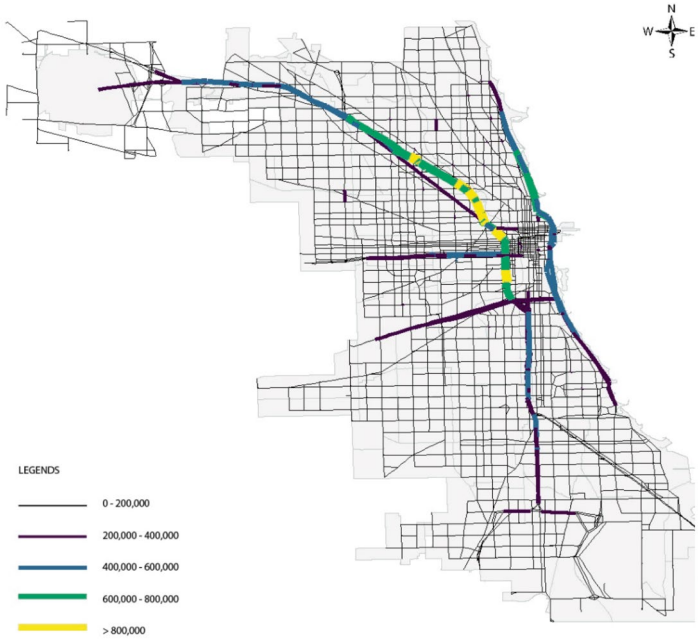

(a) Network Flow without DWC

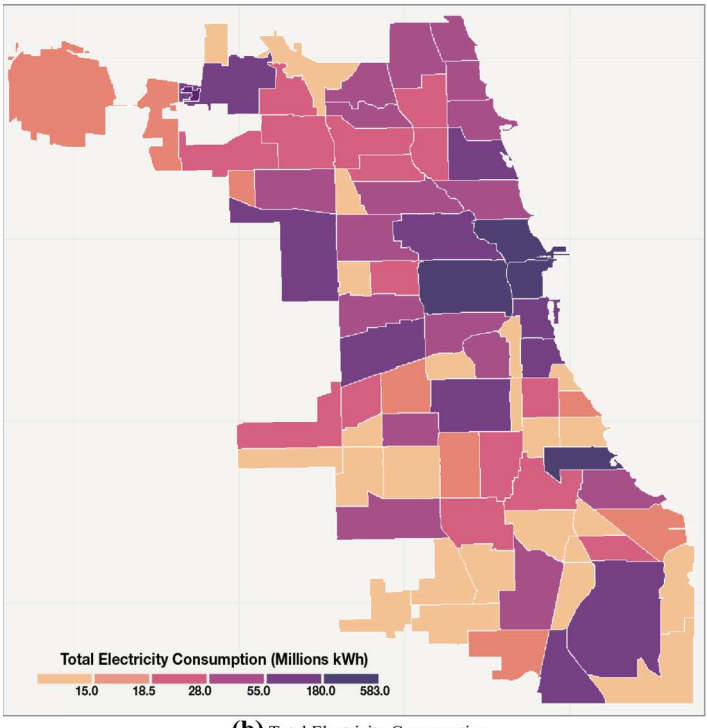

(b) Total Electricity Consumption

constraint in Eq. (8). The basic premise is each community area has limited electric power supply C_m and the model's decision on the amount of DWC shall not exceed this value. However, the investment capital applies to the entire city of Chicago as a whole and there is no regional community budget constraint.

The revised City of Chicago network used in this study consists of 2,514 nodes, of which 304 are Origin–Destination nodes, 7,393 links, and 86,661 Origin–Destination pairs with non-zero demand, and a demand of 240,340 trips. It is important to first consider the current traffic flow and the electricity consumption of the network. Figure 5a shows the base network flows, and the line color and thickness represent the amount of traffic flow on a link under no DWC scenario. Figure 5b shows the sum of domestic, industrial, and commercial electricity consumption by community area before DWC implementation.

We first apply user equilibrium traffic assignment to compute base traffic flow prior to DWC implementation. The base flow helps us identify which links are highly utilized. As expected, all three highways I90, I55, and I295 experience a higher flow due to its higher capacity than major and minor roads. In addition, the South Lake Shore Drive which runs North–South of city also has high flow.

With a population of nearly three million, the electricity demand of Chicago must also be considered when implementing DWC charging. The areas at which the total energy consumption for non-transportation (domestic, commercial and industrial) purposes is high should not be overloaded with more electricity demand from DWC implementation because it could result in a costly power outage. We gather the electricity consumption of the city as publicized in the year of 2010 (City of Chicago Energy Usage 2010) and calculate the aggregate sum of total electricity consumption measured in Millions kWh within each community area. As shown in Fig. 5b, electricity consumption is highest in the CBD area which consists of the following community areas: the Loop, Near West Side, Near North Side, and Near South Side. These areas have a high population density, multiple offices and commercial retail spaces and thus results in a high demand for electricity. However, Woodlawn, which locates in the outer borough, also experiences high electricity consumption. The area is adjacent to the University of Chicago which accounts for this high demand.

5.2 Model Output and Insights

The results of TSTT and TSEC model implementation for the Chicago city network for DWC facility location are shown in Fig. 6a, b respectively. In the lower-level solution at convergence of bi-level problem of the Chicago network case study, there was 1,779,116 paths generated for 86,950 OD pairs which results on average 20.5 paths generated per OD pair at convergence for the TSTT model. The TSEC's model are 1,833,449 paths and on average 21.1 paths per OD pair. The location and length of DWC in Fig. 6 are represented by the link color and thickness. In the TSTT model, DWC facilities are well distributed throughout the network with a focus on primary functional roadway classes such as interstates and arterials, but the local roads also receive some DWC. For major arterials, DWC facilities are implemented in a continuous manner whereas in local roads, a scattered approach is suggested.

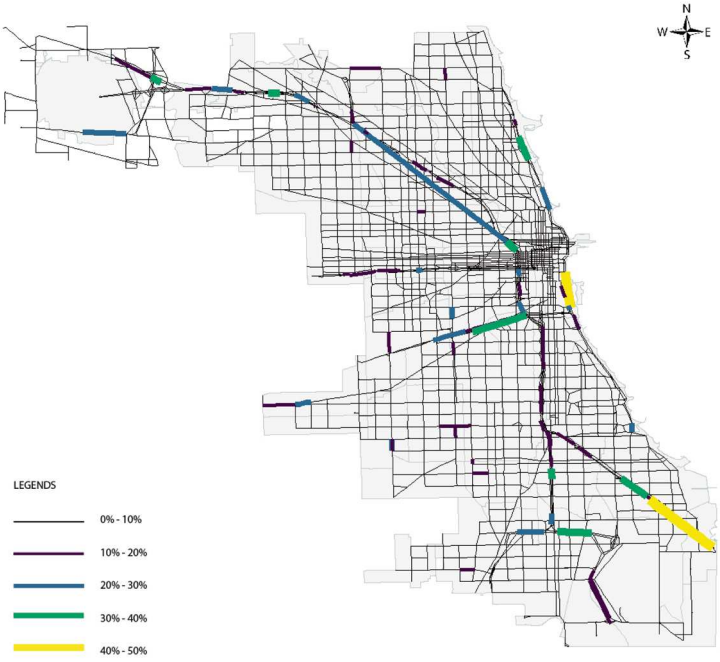

(a) DWC Location for TSTT

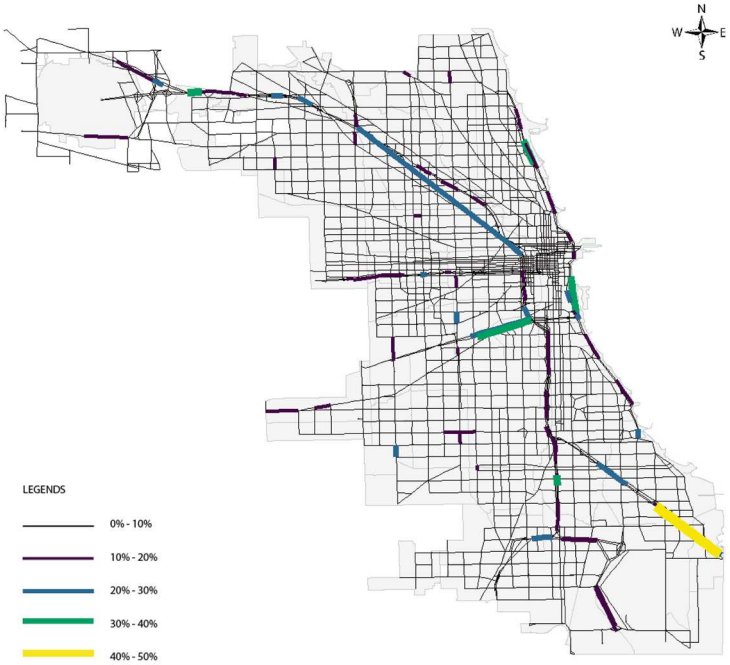

(b) DWC Location for TSEC

Fig. 6 DWC Plan for Chicago Network

The TSEC model follows a similar, but a distinctly different DWC implementation pattern as compared to the TSTT model. This is due to the predominant effect of two important constraints namely, limited failed paths and electricity distribution constraints. These two constraints narrow down the feasible region of the solution to the extent that similar solution $[y_a^*]$ are optimal under both TSTT and TSEC scenarios. As these two constraints are relaxed, we will get significantly different solution set $[y_a^*]$ under TSTT and TSEC scenarios. The majority of the DWC facilities are implemented on the following interstate highways and arterials: Interstate 90, 94, 290, 55, The S. Lake Shore Drive, and North Milwaukee Avenue. These roads share three common characteristic which are (1) higher capacity, (2) providing access from outer boroughs to the CBD area, (3) and experiencing a higher traffic flow than other roads. In addition, the majority of the available path go through these roads which is preferable for the model since these are considered more cost-effective in satisfying the limited failed path constraint. Along these for major arterials and the local roads suggested DWC implementation are sparse and well-distributed among electrical districts because of two main reasons: providing additional local DWC charging for each region and not overloading any area with DWC facility which would raise an excessive electricity demand and ultimate power shortage.

An interesting observation is that both North Milwaukee Avenue and Interstate 90 receives significant DWC treatment although North Milwaukee Avenue receives slightly more DWC than Interstate 90. This model outcome can be attributed to two main reasons: first, N. Milwaukee can be easily accessed compared to its counterpart and second, Interstate 90 already receives DWC treatment in the southern part and the loop area. Another observation is that the CBD district area receives little to none DWC treatment. It may be due the fact that if DWC facility is implemented in this area, it would attract more driver and the area would be overcrowded. Furthermore, the area has a high electricity demand and thus implementing DWC would only put more stress on the already constrained electric distribution system in that area.

In addition to the location and length of DWC for the entire network as shown in Fig. 6, it may be also beneficial for the city council to know the DWC Plan's impact on a level of community area (districts). TABLE 1 shows the detail information for the top 25 community areas ranked by the amount of investment. For each community area, the table shows the amount of money invested in, the number of failed trips avoided as a percentage of the original failed trips before DWC Implementation, the total energy provided to BEV by DWC (system energy recharged), and average speed. The number of failed trips of a community area is calculated based on the trips originated within that community area and regardless of their destinations. BEV drivers may not necessarily benefit from the DWC implemented within their community area, but they may benefit from DWC in other areas. This can partially explain for the low correlation between the amount of investment made and the avoided fail trips. The system energy recharged is calculated by taking the aggregate sum of energy recharged by all BEVs traveling within the area and this parameter has a positive relationship with the amount of investment made.

In addition, we compute the differences in travel time and total vehicle energy recharged by each road segment between the TSTT and TSEC models as shown in

Table 1 Top 20 Community Area DWC Implementation

Area Numbers	Community Area	TSTT				TSEC			
		Investment	Avoided Fail Trip	Energy Recharged (Vehicle. kWh)	Speed (mph)	Investment	Avoided Fail Trip	Energy Recharged (Vehicle. kWh)	Speed (mph)
28	NEAR WEST SIDE	$ 4,071,016	79%	2,280,478	9.6	$4,070,918	77%	2,288,102	9.1
31	LOWER WEST SIDE	$ 3,909,432	79%	1,462,183	11.1	$4,261,913	78%	1,518,896	9.5
76	OHARE	$ 3,699,190	40%	573,240	4.2	$4,184,445	45%	854,305	49.2
69	GREATER GRAND CROSSING	$ 3,579,716	83%	1,160,939	39.1	$2,989,588	81%	1,138,975	40.4
33	NEAR SOUTH SIDE	$ 3,026,728	81%	1,585,666	15.6	$2,998,306	80%	1,573,468	12.8
10	NORWOOD PARK	$ 2,953,685	78%	1,208,663	15.9	$2,481,583	80%	973,333	15.6
49	ROSELAND	$ 2,786,528	80%	550,839	18.5	$2,321,705	77%	403,178	18.5
3	UPTOWN	$ 2,767,608	72%	1,226,561	20.4	$2,718,683	70%	1,143,447	17.7
16	IRVING PARK	$ 2,611,767	86%	1,235,617	22.4	$2,341,632	87%	1,128,331	20.1
58	BRIGHTON PARK	$ 2,310,343	82%	406,321	9.7	$1,644,768	83%	272,264	9.7
48	CALUMET HEIGHTS	$ 2,295,233	84%	142,895	3.2	$3,142,935	71%	254,348	49.2
56	GARFIELD RIDGE	$ 2,275,262	68%	177,878	74.0	$2,313,931	67%	161,786	74.0
25	AUSTIN	$ 2,110,649	64%	292,621	51.2	$1,803,011	66%	258,603	53.7
65	WEST LAWN	$ 2,029,954	69%	314,048	18.9	$2,113,694	70%	323,284	18.9
44	CHATHAM	$ 1,966,609	87%	697,066	16.6	$2,169,400	83%	772,149	16.6
27	EAST GARFIELD PARK	$ 1,923,456	62%	599,488	8.4	$1,914,753	56%	604,378	8.0
11	JEFFERSON PARK	$ 1,553,835	70%	755,784	9.3	$1,536,568	72%	735,046	9.3
21	AVONDALE	$ 1,524,490	89%	1,147,426	9.5	$1,626,765	88%	1,213,164	9.5

Table 1 (continued)

Area Numbers	Community Area	TSTT				TSEC			
		Investment	Avoided Fail Trip	Energy Recharged (Vehicle. kWh)	Speed (mph)	Investment	Avoided Fail Trip	Energy Recharged (Vehicle. kWh)	Speed (mph)
22	LOGAN SQUARE	$ 1,383,665	84%	872,805	7.1	$1,087,476	84%	631,093	7.1
8	NEAR NORTH SIDE	$ 1,297,574	77%	762,868	11.6	$1,277,179	75%	725,691	11.6
37	FULLER PARK	$ 1,221,609	100%	454,164	5.2	$1,313,838	100%	489,548	5.2
66	CHICAGO LAWN	$ 1,207,145	72%	146,624	7.5	$1,308,755	66%	163,802	7.5
23	HUMBOLDT PARK	$ 1,201,371	70%	148,283	5.9	$1,197,755	66%	145,082	5.9
45	AVALON PARK	$ 1,195,053	83%	133,268	39.1	$1,134,916	77%	118,107	39.1
68	ENGLEWOOD	$ 1,193,158	72%	202,025	14.6	$1,185,177	69%	192,300	14.8

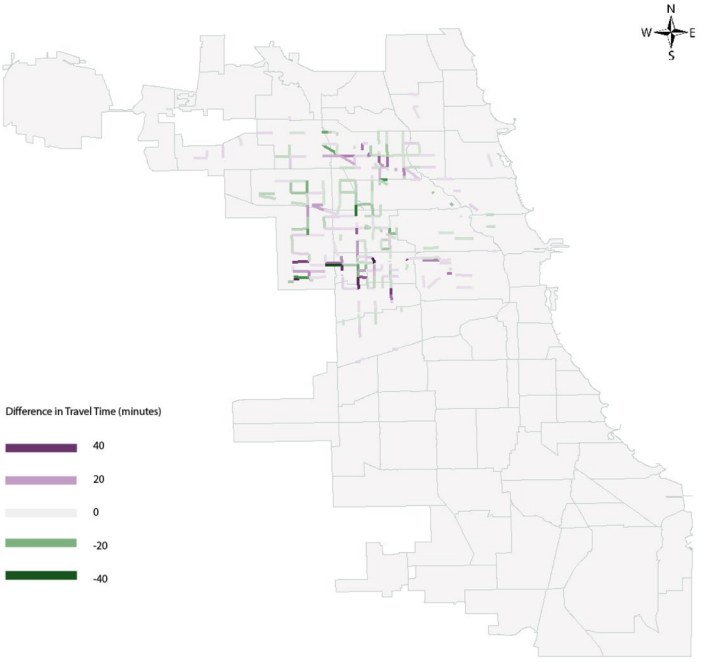

(a) Difference in Travel Time between TSTT and TSEC models

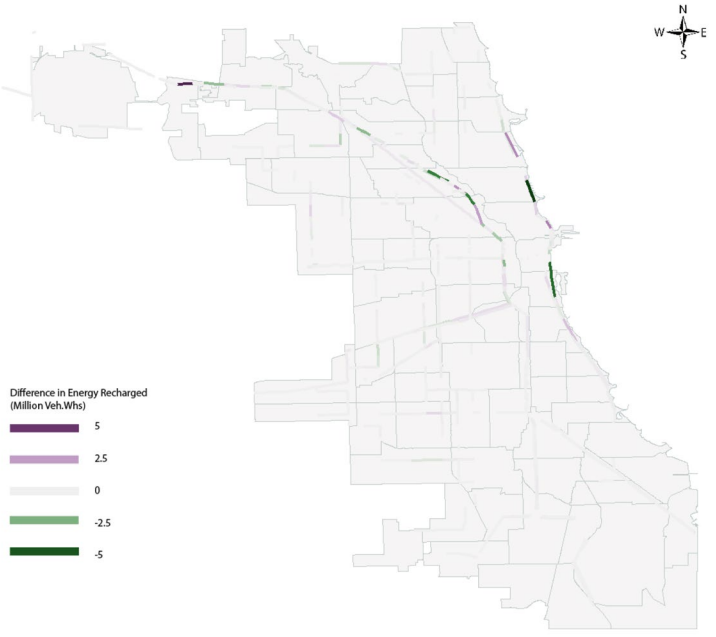

(b) Difference in Energy Recharged between TSTT and TSEC models

Fig. 7 Comparison between TSTT and TSEC model outputs

Fig. 7a, b below. The difference is plotted by a diverging color scale where the color blue indicates a net negative (TSTT's value is less than that of TSEC), white represents equal, and red represents the net positive. In Fig. 7a, we notice the difference in travel time occur mainly on the minor arterial and TSTT model has 948 min less in total network travel time compared to TSEC. This can be attributed to the reasoning behind TSTT model where it locates DWC facilities in a disperse manner. Therefore, in the lower-level user equilibrium, there's no particular path or road segment that has inherently high DWC so that high volume of vehicle would not be drawn into any particular road. This results in a more stable travel time across the network and results in a net lower travel time. In contrast, as shown in Fig. 7b, we see that the difference in energy consumption occurs mainly on highways and arterials. TSEC records a net 4.25 million Vehicle Wh of energy recharged. TSEC tends to greedily implement more DWC on highly occupied links as to maximize the total energy recharged.

6 Conclusion

In this research, we develop a modeling framework for optimally locating DWC facilities in a road network under energy availability and budget constraint that endeavors to avoid failed trips of BEVs. The proposed modeling framework can benefit city officials in developing a DWC implementation plan for their jurisdiction. A bi-level approach is proposed which encapsulates both the objectives of the planner and users. In the Upper Level, two objectives namely Total System Travel Time and Total System Energy Consumption of the planner are achieved. In the Lower-Level, the network flows are computed using user equilibrium principle where all BEV drivers are on the path yielding the minimum value of the normalized cost. Normalized cost is a combination of travel time and energy recharged by traveling through DWC facilities. The bi-level framework prompts the problem of a black box and computational heavy objective function. The research modifies and extends upon the algorithm ConstrLMSRS developed by Regis (Regis 2011).

First, the modeling framework is tested on a small network as a validation of the concept. Then, the modeling framework is applied as a case study using a real-world Chicago City network from Illinois, USA. For applicability to real-size networks, selected constraints from the original model were modified to better reflect the practical circumstances related to the availability of budget and electricity. The results suggest that major highways and arterials should be implemented with DWC because those links contribute to the majority of the trips. In addition, local roads located in outer borough also receive DWC treatment in sparse manner to adequately recharge the vehicle. However, numerical results suggest that roads located in dense areas should not be implemented with DWC. This is intuitive as otherwise it would attract more traffic to already congested area and lead to surge in electricity demand due to DWC that is already experiencing high non-transportation (domestic, commercial, industrial) electricity demand. Although this research can benefit planers in present form, it can be improved in several ways. The current model considers only one level of recharging method which is DWC and the inclusion of other methods

such as static charging, battery swapping can improve the flexibility and the diversity of the model. In the Lower Level, the traffic assignment task can incorporate other types of vehicles in addition to BEVs. Incorporation of these aspects can form interesting future extensions of this study.

We have assumed single user class with separable cost function, which implies that the cost of a link depends on the flow of that link only. Although, in this paper, the cost has two components, which includes travel time as the positive cost and the BEV charging as the negative cost, both of these components will depend on the congestion level and properties of that link only. Hence in our formulation, we do not have the asymmetric cost function and mathematical programing formulation can be used. However, incorporation of nonlinear complementarity formulation can be explored in the future as a potential candidate for representing the lower-level problem.

Data Availability The data for the Sioux Fall and Chicago network in Sects. 4.1 and 5.1 are made available via the following repository:https://github.com/hhngo96/bev. The repository contains the network configuration, origin–destination demand, and the DWC implementation plan for the TSTT model. The exact algorithm for both the upper and lower level can be provided upon request at hhngo@memphis.edu and amit.kumar@utsa.edu.

Declarations

Conflict of Interest All authors declare that they have no conflicts of interest.

References

Agrawal S, Zheng H, Peeta S, Kumar A (2016) Routing aspects of electric vehicle drivers and their effects on network performance. Transp Res Part Transp Environ 46:246–266

Ben-Ayed O, Blair CE (1990) Computational difficulties of bilevel linear programming. Oper Res 38:556–560

Boyce DE, Chon KS, Ferris ME, Lee YJ, Lin K-T, Eash RW (1985) Implementation and evaluation of combined models of urban travel and location on a sketch planning network. Chic Area Transp Study

Burgess EW, Newcomb C (1920) Census data of the city of Chicago. The University of Chicago Press, Chicago

Chen Z, He F, Yin Y (2016) Optimal deployment of charging lanes for electric vehicles in transportation networks. Transp Res Part B Methodol 91:344–365. https://doi.org/10.1016/j.trb.2016.05.018

City of Chicago Energy Usage 2010 | City of Chicago | Data Portal. https://data.cityofchicago.org/Environment-Sustainable-Development/Energy-Usage-2010/8yq3-m6wp. Accessed 30 Jul 2019

Deng X (1998) Complexity issues in bilevel linear programming. In: Multilevel optimization: Algorithms and applications. Springer, pp 149–164

Dong J, Liu C, Lin Z (2014) Charging infrastructure planning for promoting battery electric vehicles: An activity-based approach using multiday travel data. Transp Res Part C Emerg Technol 38:44–55. https://doi.org/10.1016/j.trc.2013.11.001

Fuller M (2016) Wireless charging in California: Range, recharge, and vehicle electrification. Transp Res Part C Emerg Technol 67:343–356. https://doi.org/10.1016/j.trc.2016.02.013

García-Vázquez CA, Llorens-Iborra F, Fernández-Ramírez LM et al (2017) Comparative study of dynamic wireless charging of electric vehicles in motorway, highway and urban stretches. Energy 137:42–57. https://doi.org/10.1016/j.energy.2017.07.016

Haque K, Mishra S, Golias MM (2021) Multi-period transportation network investment decision making and policy implications using econometric framework. Res Transp Econ 89:101109

He F, Yin Y, Zhou J (2015) Deploying public charging stations for electric vehicles on urban road networks. Transp Res Part C Emerg Technol 60:227–240. https://doi.org/10.1016/j.trc.2015.08.018
He J, Yang H, Huang H-J, Tang T-Q (2018) Impacts of wireless charging lanes on travel time and energy consumption in a two-lane road system. Phys Stat Mech Its Appl 500:1–10. https://doi.org/10.1016/j.physa.2018.02.074
Huang, Y., Li, S., & Qian, Z. S. (2015). Optimal deployment of alternative fueling stations on transportation networks considering deviation paths. Networks and Spatial Economics, 15, 183-204.
Huang Y, Li S, Qian ZS (2015) Optimal deployment of alternative fueling stations on transportation networks considering deviation paths. Netw Spat Econ 15:183–204
Hwang I, Jang YJ, Ko YD, Lee MS (2018) System optimization for dynamic wireless charging electric vehicles operating in a multiple-route environment. IEEE Trans Intell Transp Syst 19:1709–1726. https://doi.org/10.1109/TITS.2017.2731787
Jang YJ (2018) Survey of the operation and system study on wireless charging electric vehicle systems. Transp Res Part C Emerg Technol 95:844–866. https://doi.org/10.1016/j.trc.2018.04.006
Kitthamkesorn S, Chen A (2017) Alternate weibit-based model for assessing green transport systems with combined mode and route travel choices. Transp Res Part B Methodol 103:291–310. https://doi.org/10.1016/j.trb.2017.04.011
Koh A (2007) Solving transportation bi-level programs with Differential Evolution. IEEE Congr Evol Comput 2243–2250
Kuby M, Lim S (2005) The flow-refueling location problem for alternative-fuel vehicles. Socioecon Plann Sci 39:125–145
Kumar A, Peeta S (2014a) Slope-based path shift propensity algorithm for the static traffic assignment problem. Int J Traffic Transp Eng 4:297–319
Kumar A, Peeta S (2014b) Strategies to enhance the performance of path-based static traffic assignment algorithms. Comput-Aided Civ Infrastruct Eng 29:330–341
Kumar A, Peeta S, Nie Y (2012) Update strategies for restricted master problems for user equilibrium traffic assignment problem: computational study. Transp Res Rec 2283:131–142
Kumar A, Mishra S (2018) A simplified framework for sequencing of transportation projects considering user costs and benefits. Transp Transp Sci 14(4):346–371
Kumar A, Haque K, Mishra S, Golias MM (2019) Multi-criteria based approach to identify critical links in a transportation network. Case Stud Transp Policy 7(3):519–530
Lau TW, Chung CY, Wong KP et al (2009) Quantum-inspired evolutionary algorithm approach for unit commitment. IEEE Trans Power Syst 24:1503–1512. https://doi.org/10.1109/TPWRS.2009.2021220
Leblanc LJ (1975) An algorithm for the discrete network design problem. Transp Sci 9:183–199. https://doi.org/10.1287/trsc.9.3.183
Lee Y-G, Kim H-S, Kho S-Y, Lee C (2014) User equilibrium-based location model of rapid charging stations for electric vehicles with batteries that have different states of charge. Transp Res Rec J Transp Res Board 2454:97–106. https://doi.org/10.3141/2454-13
Liu H, Wang DZW (2017) Locating multiple types of charging facilities for battery electric vehicles. Transp Res Part B Methodol 103:30–55. https://doi.org/10.1016/j.trb.2017.01.005
Liu J, Wang X, Khattak A (2016) Customizing driving cycles to support vehicle purchase and use decisions: Fuel economy estimation for alternative fuel vehicle users. Transp Res Part C Emerg Technol 67:280–298. https://doi.org/10.1016/j.trc.2016.02.016
Liu Z, Song Z (2017) Robust planning of dynamic wireless charging infrastructure for battery electric buses. Transp Res Part C Emerg Technol 83:77–103
Liu Z, Song Z, He Y (2017) Optimal deployment of dynamic wireless charging facilities for an electric bus system. Transp Res Rec 2647:100–108
Los M, Lardinois C (1982) Combinatorial programming, statistical optimization and the optimal transportation network problem. Transp Res Part B Methodol 16:89–124
Matisziw TC (2019) Maximizing expected coverage of flow and opportunity for diversion in networked systems. Netw Spat Econ 19:199–218
Montoya A, Guéret C, Mendoza JE, Villegas JG (2017) The electric vehicle routing problem with nonlinear charging function. Transp Res Part B Methodol 103:87–110. https://doi.org/10.1016/j.trb.2017.02.004
Ngo H, Kumar A, Mishra S (2020) Optimal positioning of dynamic wireless charging infrastructure in a road network for battery electric vehicles. Transp Res Part D Transp Environ 85:102385

Panchal C, Stegen S, Lu J (2018) Review of static and dynamic wireless electric vehicle charging system. Eng Sci Technol Int J 21:922–937. https://doi.org/10.1016/j.jestch.2018.06.015

Pishvaee MS, Farahani RZ, Dullaert W (2010) A memetic algorithm for bi-objective integrated forward/reverse logistics network design. Comput Oper Res 37:1100–1112. https://doi.org/10.1016/j.cor.2009.09.018

Regis RG (2011) Stochastic radial basis function algorithms for large-scale optimization involving expensive black-box objective and constraint functions. Comput Oper Res 38:837–853. https://doi.org/10.1016/j.cor.2010.09.013

Riemann R, Wang DZW, Busch F (2015) Optimal location of wireless charging facilities for electric vehicles: Flow-capturing location model with stochastic user equilibrium. Transp Res Part C Emerg Technol 58:1–12. https://doi.org/10.1016/j.trc.2015.06.022

Sathaye N, Kelley S (2013) An approach for the optimal planning of electric vehicle infrastructure for highway corridors. Transp Res Part E Logist Transp Rev 59:15–33. https://doi.org/10.1016/j.tre.2013.08.003

Sheffi Y (1985) Urban transportation networks: Equilibrium analysis with mathematical programming methods. Prentice Hall

Strehler M, Merting S, Schwan C (2017) Energy-efficient shortest routes for electric and hybrid vehicles. Transp Res Part B Methodol 103:111–135. https://doi.org/10.1016/j.trb.2017.03.007

USDOE (2018) Alternative Fuels Data Center: Electric Vehicle Charging Station Locations. https://www.afdc.energy.gov/fuels/electricity_locations.html#/analyze?show_private=true&show_planned=true. Accessed 25 Jul 2018

Xie C, Wang T-G, Pu X, Karoonsoontawong A (2017) Path-constrained traffic assignment: Modeling and computing network impacts of stochastic range anxiety. Transp Res Part B Methodol 103:136–157. https://doi.org/10.1016/j.trb.2017.04.018

Zhang A, Kang JE, Kwon C (2017) Incorporating demand dynamics in multi-period capacitated fast-charging location planning for electric vehicles. Transp Res Part B Methodol 103:5–29. https://doi.org/10.1016/j.trb.2017.04.016

Zhang X, Rey D, Waller ST, Chen N (2019) Range-constrained traffic assignment with multi-modal recharge for electric vehicles. Netw Spat Econ 19:633–668

Zheng H, He X, Li Y, Peeta S (2017) Traffic equilibrium and charging facility locations for electric vehicles. Netw Spat Econ 17:435–457

Authors and Affiliations

Amit Kumar[1] · Sabyasachee Mishra[2] · Huan Ngo[2]

✉ Amit Kumar
amit.kumar@utsa.edu

Sabyasachee Mishra
smishra3@memphis.edu

Huan Ngo
hhngo@memphis.edu

[1] Department of Civil and Environmental Engineering, University of Texas at San Antonio, One UTSA Circle, San Antonio, TX 78249, USA

[2] Department of Civil Engineering, University of Memphis, 104 Engineering Science Building, Memphis, TN 38152, USA